HHS Public Access

Author manuscript

Circ Res. Author manuscript; available in PMC 2024 May 26.

Published in final edited form as:

Circ Res. 2023 May 26; 132(11): e206–e222. doi:10.1161/CIRCRESAHA.122.322473.

A Critical Role for ERO1α in Arterial Thrombosis and Ischemic Stroke

Vishwanath Jha[1,#], **Bei Xiong**[1,2,#], **Tripti Kumari**[1], **Gavriel Brown**[1], **Jinzhi Wang**[1], **Kyungho Kim**[3], **Jingu Lee**[1], **Nathan Asquith**[4,5], **John Gallagher**[1], **Lillian Asherman**[1], **Taylor Lambert**[1], **Yanyan Bai**[6], **Xiaoping Du**[6], **Jeong-Ki Min**[7], **Rajan Sah**[8,9], **Ali Javaheri**[8], **Babak Razani**[8,9,10], **Jin-Moo Lee**[11,12,13,14], **Joseph E. Italiano**[4,5], **Jaehyung Cho**[1,10]

[1]Division of Hematology, Department of Medicine, Washington University School of Medicine, St. Louis, MO 63110, USA

[2]Department of Hematology, Zhongnan Hospital of Wuhan University, Wuhan, Hubei, P.R. China

[3]Korean Medicine-Application Center, Korea Institute of Oriental Medicine, Daegu, Republic of Korea

[4]Department of Medicine, Harvard Medical School, Boston, MA 02115, USA

[5]Vascular Biology Program, Boston Children's Hospital, Boston, MA 02115, USA

[6]Department of Pharmacology and Regenerative Medicine, The University of Illinois at Chicago College of Medicine, IL 60612, USA

[7]Biotherapeutics Translational Research Center, Korea Research Institute of Bioscience and Biotechnology, Daejeon, Republic of Korea

[8]Cardiovascular Division, Department of Medicine, Washington University School of Medicine, St. Louis, MO 63110, USA

[9]John Cochran VA Medical Center, St. Louis, MO 63106, USA

[10]Department of Pathology and Immunology, Washington University School of Medicine, St. Louis, MO 63110, USA

[11]Department of Neurology, Washington University School of Medicine, St. Louis, MO 63110, USA

[12]Hope Center for Neurological Disorders, Washington University School of Medicine, St. Louis, MO 63110, USA

Correspondence: Jaehyung Cho, Ph.D., 660 S. Euclid Ave, Campus Box 8125, St. Louis, MO 63110, jaehyung.cho@wustl.edu / Tel: 314-362-8804.

[#]These authors contributed equally to this study.

Disclosures

The authors declare no conflict of interest.

Supplementary Material

Supplemental Methods

Figure S1 to S17

Table S1

Data file S1 to S2

Movie S1 to S6

[13]Mallinckrodt Institute of Radiology, Washington University School of Medicine, St. Louis, MO 63110, USA

[14]Department of Biomedical Engineering, Washington University School of Medicine, St. Louis, MO 63110, USA

Abstract

BACKGROUND: Platelet adhesion and aggregation play a crucial role in arterial thrombosis and ischemic stroke. Here we identify platelet endoplasmic reticulum oxidoreductase 1α (ERO1α) as a novel regulator of Ca^{2+} signaling and a potential pharmacological target for treating thrombotic diseases.

METHODS: Intravital microscopy, animal disease models, and a wide range of cell biological studies were utilized to demonstrate the pathophysiological role of ERO1α in arteriolar and arterial thrombosis and to prove the importance of platelet ERO1α in platelet activation and aggregation. Mass spectrometry, electron microscopy, and biochemical studies were employed to investigate the molecular mechanism. We used novel blocking antibodies and small molecule inhibitors to study whether ERO1α can be targeted to attenuate thrombotic conditions.

RESULTS: Megakaryocyte-specific or global deletion of Ero1α in mice similarly reduced platelet thrombus formation in arteriolar and arterial thrombosis without affecting tail bleeding times and blood loss following vascular injury. We observed that platelet ERO1α localized exclusively in the dense tubular system and promoted Ca^{2+} mobilization, platelet activation, and aggregation. Platelet ERO1α directly interacted with stromal interaction molecule 1 (STIM1) and sarco/endoplasmic reticulum Ca^{2+}-ATPase 2 (SERCA2) and regulated their functions. Such interactions were impaired in mutant STIM1-Cys49/56Ser and mutant SERCA2-Cys875/887Ser. We found that ERO1α modified an allosteric Cys49-Cys56 disulfide bond in STIM1 and a Cys875-Cys887 disulfide bond in SERCA2, contributing to Ca^{2+} store content and increasing cytosolic Ca^{2+} levels during platelet activation. Inhibition of Ero1α with small molecule inhibitors but not blocking antibodies attenuated arteriolar and arterial thrombosis and reduced infarct volume following focal brain ischemia in mice.

CONCLUSIONS: Our results suggest that ERO1α acts as a thiol oxidase for Ca^{2+} signaling molecules, STIM1 and SERCA2, and enhances cytosolic Ca^{2+} levels, promoting platelet activation and aggregation. Our study provides evidence that ERO1α may be a potential target to reduce thrombotic events.

Graphical Abstract

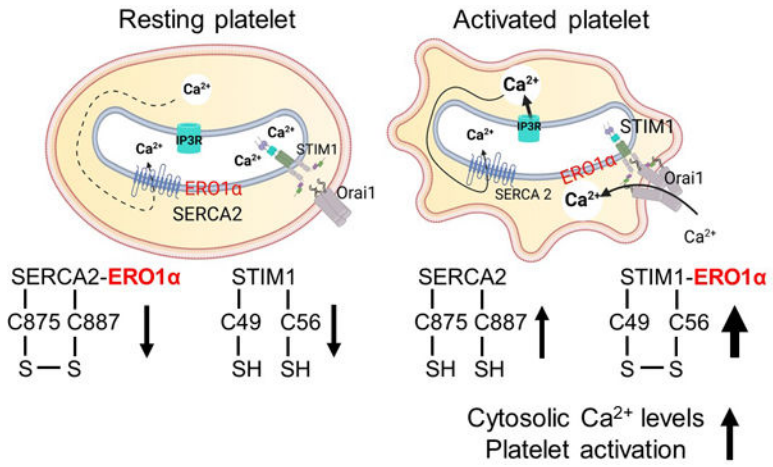

Thrombotic and thromboinflammatory diseases, including atherothrombosis and ischemic stroke, are the leading cause of death in the US. Although many antiplatelet and anti-inflammatory therapies targeting signaling molecules or receptor-ligand interactions have been used for disease treatment, these drugs increase the risk of major bleeding and impair immune responses. Thus, there is a need for additional antithromboinflammatory therapeutics. Our study reveals novel functions of platelet ERO1α in regulating Ca^{2+} signaling and platelet activation during the pathogenesis of arterial thrombosis and ischemic stroke. Unlike previous reports, we have found that platelet ERO1α is not released or detected on the platelet surface, but it is localized in the organelle where Ca^{2+} is stored. Upon platelet activation, ERO1α interacts with Ca^{2+} signaling molecules and regulates intracellular Ca^{2+} levels. Using mouse studies with a novel ERO1α inhibitor identified by a high throughput screen, we demonstrate that inhibition of Ero1α effectively attenuates arterial thrombosis and tissue damage in ischemic stroke without impairing bleeding times.

Keywords

Platelets; Basic Science Research; Cell Signaling/Signal Transduction; Mechanisms; Translational Studies; ERO1α; arterial thrombosis; ischemic stroke; platelet activation; Ca^{2+} mobilization

INTRODUCTION

Arterial thrombotic diseases, including coronary artery disease and ischemic stroke, result in >30% of all deaths globally.[1] Underlying these pathologies is increased platelet activity. After arterial injury, platelets adhere to collagen and von Willebrand factor (vWF) through glycoprotein VI (GPVI) and the GPIb-IX-V complex, respectively, and aggregate through the interaction between fibrinogen and activated αIIbβ3 integrin, resulting in vaso-occlusive thrombosis.[2] Furthermore, a similar mechanism occurs after tissue injury to stop bleeding. Therefore, platelets are essential for thrombosis and hemostasis. Although the diverse ligand-receptor interactions trigger different signaling pathways during platelet activation, they all increase cytosolic Ca^{2+} levels. Like other cell types,[3] platelet stromal interaction molecule 1 (STIM1) has an essential role in detecting Ca^{2+} depletion in the dense tubular system (DTS) and activating store-operated Ca^{2+} entry (SOCE), contributing to arterial

thrombosis and hemostasis.[4] Reuptake of Ca^{2+} into the DTS is mediated by sarco/ER Ca^{2+} ATPases (SERCAs), and STIM1 also contributes to SERCA-mediated Ca^{2+} store refilling in activated platelets.[5] Current anti-platelet therapies blocking a signaling molecule or a ligand-receptor interaction reduce the morbidity and mortality associated with thrombotic disease, but they increase the risk of major bleeding.[6] Therefore, many efforts have been made to identify a novel therapeutic target for a safer anti-platelet agent.

We and others have demonstrated that targeting extracellular protein disulfide isomerase (PDI) might be a therapeutic strategy for treating thrombotic disease.[7–9] However, treatment with blocking anti-PDI antibodies prolongs bleeding times and increases blood loss at the site of tail amputation in mice,[7] raising a concern that selective PDI inhibitors may perturb hemostatic function. Moreover, cell-permeable PDI inhibitors may cause serious side effects due to the indispensable role of PDI in protein folding in the ER and cell viability.[10,11] Endoplasmic reticulum oxidoreductase 1 (ERO1) oxidizes PDI via a disulfide bond exchange during oxidative protein folding.[11] Of the two isoforms found in mammalian cells, ERO1α is ubiquitously expressed,[12] whereas ERO1β is predominantly found in intestinal and pancreatic β-cells.[13,14] Unlike mice lacking *Pdi*, which display embryonic lethality,[11] mice with loss-of-function mutations of *Ero1-l* and *Ero1-lβ* are viable with a moderate defect in secretory protein production,[15,16] implicating the role of ERO1 in disulfide bond oxidation as well as the presence of an ERO1-independent mechanism of protein folding.[17] A recent study shows that extracellular ERO1α-PDI forms an electron transport system, regulating platelet function.[18] However, the authors used concentrations of ERO1α and PDI (0.1–0.5 μM) which are much greater than those detected under healthy and disease conditions (around 10–100 pM),[19,20] which makes the finding physiologically inapplicable. Confocal microscopy and biochemical studies suggest that ERO1α is colocalized with PDI and αIIbβ3 on the surface of unstimulated platelets and that treatment with polyclonal anti-ERO1α antibodies abrogates platelet aggregation.[21] However, this study did not show how intracellular ERO1α is released from platelets. More importantly, none of the studies demonstrate the contribution of ERO1α to the pathology of thrombogenesis.

Using megakaryocyte-specific Ero1α conditional knockout (CKO) and global KO mice, novel blocking antibodies, and small-molecule inhibitors, we demonstrate that platelet Ero1α has a crucial role in platelet thrombus formation at the site of cremaster arteriolar and carotid arterial injuries. Immunogold electron microscopy and biochemical studies reveal that ERO1α is not released from platelets and detected on the platelet surface but is localized exclusively in the DTS. Intriguingly, ERO1α contributes to Ca^{2+} store content and promotes Ca^{2+} mobilization in a PDI-independent manner, resulting in platelet activation and aggregation. We identify STIM1 and SERCA2 as ERO1α binding partners in platelets. ERO1α interacts with the N-terminal ER luminal domain of STIM1 during platelet activation. In contrast, binding of ERO1α to SERCA2 is decreased upon agonist stimulation. Importantly, ERO1α alters a Cys49-Cys56 disulfide bond in STIM1 and a Cys875-Cys887 disulfide bond in SERCA2, regulating their functions. Treatment of mice with a novel small-molecule ERO1α inhibitor attenuates arterial thrombogenesis and infarct volume in ischemic stroke without increasing tail bleeding times. Our results provide evidence that targeting ERO1α might be an effective therapeutic strategy for treating thrombotic disease.

METHODS

Data Availability

All data and materials will be made publicly available upon publication. A detailed description of materials and methods can be found in the Supplemental Material.

Mice

WT (C57BL/6J), β3 KO, and BALB/cJ mice were obtained from The Jackson Laboratory (Bar Harbor, ME). WT control ($Pdi^{flox/flox;\ Pf4\text{-}cre^{-/-}}$) and megakaryocyte-specific Pdi CKO mice ($Pdi^{flox/flox;Pf4\text{-}cre^{+/-}}$) were generated by crossing Pf4-Cre mice with $Pdi^{flox/flox}$ mice as we reported.[8] Ero1α CKO and KO mice were generated as described in the Supplemental Method. All animal care and experimental procedures were approved by the Institutional Animal Care and Use Committee at Washington University School of Medicine. Animals were assigned randomly to the different experimental groups.

Isolation of platelets, neutrophils, and cardiac endothelial cells

Human platelets, mouse platelets, neutrophils, and cardiac endothelial cells were isolated and prepared as we described previously.[22,23]

Intravital microscopy

Intravital microscopy was performed in a mouse model of laser-induced cremaster arteriolar injury as we described.[24] WT (C57BL/6), littermate WT control, and CKO and KO male mice (8–10 weeks old) were anesthetized with intraperitoneal injection of ketamine and xylazine. The cremaster muscle was exteriorized and superfused with 37ºC bicarbonate-buffered saline throughout the experiment. Arteriolar wall injury was induced by laser ablation (Photonics Instruments) as we described.[22,24] Multiple thrombi were generated in at least 3–4 different arterioles of one mouse, with new thrombi formed upstream of earlier thrombi to minimize any contribution from thrombi generated earlier in the mouse. Platelets and fibrin were visualized by infusion of DyLight 649-conjugated anti-CD42c (0.2 μg/g BW) and Alexa Fluor 488-conjugated anti-fibrin (0.2 μg/g BW) antibodies, respectively. To detect extracellular Ero1α, Alexa Fluor 488-conjugated rabbit IgG or non-blocking anti-ERO1α antibodies (0.2 μg/g BW) were injected into WT (C57BL/6), WT control, Ero1α KO, and Ero1α CKO mice. In some experiments, wtERO1α or activity-null ERO1α-Cys94Ser (mERO1α) (4 μg/g BW) was infused into Ero1α KO mice before imaging. To test the effect of ERO1α inhibitors or blocking anti-ERO1α antibodies, WT (C57BL/6) mice were treated with intravenous injection of vehicle control, eptifibatide (5 μg/g BW), B12–5 (5 μg/g BW), isotype control IgGs, anti-ERO1α (15E9, 1–3 μg/g BW), or anti-PDI (BD34, 3 μg/g BW) 3 minutes before treatment with the anti-CD42c and anti-fibrin antibodies. The same dose of eptifibatide was injected every 20 minutes to maintain the inhibitory effect. The experiments were performed in a single-blind fashion in which the investigators did not know the identity of the sample or mouse. Fluorescence and bright-field images were captured in 6–10 different cremaster arterioles with a diameter of 30–45 μm in each mouse and recorded using either an Olympus BX61W microscope with a 60 × 1.0 NA water immersion objective or a Zeiss Axio examiner Z1 microscope system with a Yokogawa

confocal spinning disk (CSU-W1) equipped with four stack laser system (405 nm, 488 nm, 561 nm, and 637 nm wavelengths). Images were collected with a high-speed, high-resolution camera (2304 × 2304 pixel format, ORCA-Fusion BT sCMOS, Hamamatsu). Time "0" was set to when image capture began on each vessel. The data were analyzed using Slidebook (version 6.0, Intelligent Imaging Innovations). Due to the significant variation between vessels in the same mouse, the result from each vessel was counted as an individual value. Representative images were chosen that most closely resemble the mean values in the quantifications.

Ca^{2+} mobilization

Ca^{2+} mobilization was measured as described previously.[25] WT control and Ero1α-null platelets (1×10^8/ml) were suspended in HEPES-Tyrode buffer, pH 7.4. Cells were incubated with a Ca^{2+} dye (FLIPR Ca^{2+} 5 Assay kit, Molecular Devices) for 30 minutes at 37°C in the dark, followed by stimulation with thrombin (0.1 U/ml), A23187 (2 μM), or thapsigargin (10–20 μM). After measuring Ca^{2+} release, 1 mM $CaCl_2$ was immediately added to assess Ca^{2+} influx. In other experiments, Ca^{2+} dye-labeled human and WT mouse platelets were incubated with a vehicle or an inhibitor for 10 minutes at 37°C. Cytosolic Ca^{2+} levels were measured using a FlexStation3 microplate reader with an excitation wavelength of 485 nm and an emission wavelength of 525 nm. Ca^{2+} mobilization was quantified by the area under the curve (AUC) and expressed as a relative fluorescence unit.

Statistical analysis

Detailed statistical methods were specified in the figure legends. For comparisons of two groups, unpaired two-tailed Student's *t*-test or Mann-Whitney U test (for non-normally distributed data) was used. For one-way parametric tests, one-way ANOVA with Dunnett's or Tukey's multiple comparison tests were used. For one-way nonparametric tests, Kruskal-Wallis test with Dunn's multiple comparison tests were used. GraphPad Prism 9 (version 9.5.1) was used for statistical analysis.

RESULTS

Ero1α has a crucial role in platelet thrombus formation after cremaster arteriolar and carotid arterial injuries but does not affect tail bleeding times in mice

Platelet PDI has an important role in arterial thrombosis and ischemic stroke.[8,22,26] However, it is unclear how platelet PDI activity is regulated in thrombosis. Thus, we sought to identify molecules that interact with PDI and may regulate its activity during platelet activation. We immunoprecipitated PDI in lysates of resting and thrombin-activated human platelets and conducted mass spectrometry. PDI interacted with many intracellular and surface molecules, including UDP-glucose GP glucosyltransferase 1, serpins, ERO1α, β3 integrin, and GPIbα (Figure S1A and Data file S1). Among them, ERO1α attracted our interest (Figure S1B–C) as it is a known ER oxidase of PDI.[27] We verified that PDI interacted with ERO1α, and the interaction was decreased during platelet activation (Figure S1D).

Since ERO1α has been reported to colocalize with PDI and αIIbβ3 integrin on the platelet surface,[21] we performed intravital microscopy to detect extracellular Ero1α at the site of laser-induced cremaster arteriolar injury in mice.[22] Using fluorescently labeled non-blocking polyclonal anti-ERO1α antibodies,[28] we found that Ero1α accumulated at the site of laser-induced cremaster arteriolar injury (Figure 1A–C and Movies 1–2). However, unlike Pdi whose accumulation is significantly reduced as the size of platelet thrombi is decreased,[7] the signal of extracellular Ero1α remained unaltered 4 minutes after laser injury. This result suggests that platelets are unlikely to be the main source of extracellular Ero1α.

To investigate the role of ERO1α in arterial thrombosis, *Ero1-l*$^{fl/fl}$ mice were generated and bred with *Pf4*-cre and *Cmv*-cre mice to delete Ero1α in megakaryocytes (Ero1α$^{fl/fl;Pf4\text{-}cre+/-}$) and all tissues (Ero1α$^{-/-;Cmv\text{-}cre+/-}$), respectively (Figure S2A–C). Ero1α KO mice were viable, fertile, and born in a normal Mendelian ratio without any abnormality, suggesting that Ero1α is dispensable for embryonic development. Megakaryocyte-specific and global deletion of Ero1α did not alter the expression of other proteins, such as Pdi, αIIbβ3 integrin, GPIbα, and GPVI (Figure S2D–H), and did not affect complete blood counts (CBC) (Tables 1–2). Intravital microscopy using the CKO and KO mice revealed that either megakaryocyte-specific or global deletion of Ero1α significantly mitigated platelet accumulation after laser-induced cremaster arteriolar injury without inhibiting initial platelet adhesion (Figure 1D–F and Movies 3–6). Fibrin generation was reduced only in Ero1α KO mice. These results indicate that platelet Ero1α mainly contributes to platelet thrombus formation, whereas other cellular Ero1α plays a role in fibrin generation. We reported that the defect in platelet thrombus formation in megakaryocyte-specific Pdi CKO mice was completely rescued by injection of recombinant wild-type PDI (wtPDI) but not its activity-null mutant.[22] However, injection of wtERO1α at 50 μg/g body weight (BW) into Ero1α KO mice exhibited a minimal rescue effect on platelet thrombus formation and fibrin generation (Figure 1G–H). Its activity-null mERO1α did not show any effect. This result suggests that extracellular Ero1α only partially contributes to thrombogenesis.

Atherothrombosis occurs after the rupture of an atherosclerotic plaque.[29] To mimic the pathological condition, we utilized a $FeCl_3$-induced carotid arterial thrombosis model, an occlusive platelet thrombus is produced by application of the $FeCl_3$-saturated filter paper to the external surface of the carotid artery.[30] Compared with WT control mice, Ero1α CKO and KO mice exhibited a significant prolongation of the time to occlusion (TTO) in the injured carotid artery (Figure 1I). Mice deficient in β3 integrin, a model of Glanzmann thrombasthenia, showed a maximal increase in TTO compared to WT mice. Importantly, megakaryocyte-specific or global deletion of Ero1α did not affect bleeding times and blood loss after amputating the tail tip, whereas deletion of β3 integrin markedly increased (Figure 1J–K). Overall, these results indicate that platelet Ero1α promotes platelet thrombus formation in arterial thrombosis and that Ero1α does not affect tail bleeding times in mice.

Intracellular ERO1α promotes platelet activation and aggregation independently of PDI

Due to the lack of inhibitory anti-ERO1α antibodies, we developed mouse monoclonal blocking antibodies against recombinant human ERO1α. After screening antisera and testing

hybridomas (Figure S3A–C), we identified the clone 15E9 that recognizes human and mouse platelet ERO1α, wtERO1α, and mERO1α, but not PDI, and inhibits the oxidase activity of ERO1α in a concentration-dependent manner (Figure S3D–G). 8B2 and 10C1 were identified as non-blocking anti-ERO1α antibodies. Flow cytometry showed no binding of 15E9 to mouse and human platelets under resting and activated conditions (Figure S4A–B). Furthermore, unlike PDI, ERO1α was not detected in the releasate from activated mouse and human platelets (Figure S4C). We have reported that approximately 32,000 PDI molecules are present in one human platelet,[22] and <10% of total PDI is released during platelet activation.[31] Given the assumption that 15E9 binds to recombinant human ERO1α and human and mouse platelet ERO1α with the same affinity, we found that one human or mouse platelet expressed approximately 2,500 or 1,800 ERO1α molecules, respectively (Figure S5).

To confirm the contribution of platelet Ero1α to thrombus formation, we performed a flow chamber assay. Blood from WT and Ero1α CKO mice was perfused over immobilized fibrillar type I collagen at an arterial shear rate (1000 s^{-1}).[22] WT platelets formed widespread thrombi on collagen surfaces, whereas Ero1α-null platelets showed a significant reduction in surface coverage and the volume of thrombi (Figure 2A). As assessed by platelet aggregation and ATP (dense granule) secretion measured simultaneously by light transmission and luminescence,[22] deletion of Ero1α significantly inhibited both events induced by various agonists, such as thrombin (0.025 U/ml), collagen-related peptides (CRP, 0.05 μg/ml), and Ca^{2+} ionophore A23187 (0.5 μM), but not ADP (2.5 μM) (Figure 2B–E). Such defects disappeared when platelets were treated with a high concentration of agonists (Figure S6). These results imply that platelet Ero1α regulates a common signaling pathway involved in Ca^{2+} signaling and granule secretion.

We reported that Pdi deletion reduces platelet aggregation, and exogenously-added wtPDI restores Pdi-null platelet aggregation to the WT level.[22] However, treatment with wtERO1α or wtPDI did not rescue the defect in Ero1α-null platelet aggregation (Figure 2F), suggesting that intracellular ERO1α promotes platelet aggregation independently of extracellular ERO1α and PDI. A recent study showed that 10–33 μM EN460, an ERO1α inhibitor (IC_{50} = 1.9 μM),[32] significantly blocks thrombin-induced platelet aggregation.[18] We found that 3–10 μM EN460 abrogated thrombin-induced aggregation of mouse and human platelets (Figure S7A–B). However, Ero1α-null platelet aggregation was also abolished by 3 μM EN460 (Figure S7C).

We reported that loss of Pdi reduces αIIbβ3 integrin activation without affecting P-selectin exposure and the interaction between talin1 and the β3 integrin subunit.[22] As measured by flow cytometry, loss of Ero1α impaired both P-selectin exposure and αIIbβ3 integrin activation in response to thrombin and CRP (Figure 2G–H). Furthermore, immunoprecipitation assays showed that talin1-β3 integrin binding was significantly reduced in thrombin-activated Ero1α-null platelets compared with WT platelets (Figure 2I). Transmission electron microscopy revealed similar ultrastructures between WT and Ero1α-null platelets (Figure 2J). Treatment with 15E9 did not affect P-selectin exposure and αIIbβ3 integrin activation in thrombin- or CRP-activated platelets (Figure S8A–B). Also, inhibition of extracellular Ero1α with 15E9 did not impair thrombin-induced aggregation of

mouse and human platelets (Figure S8C–D). In contrast, treatment with a blocking anti-PDI antibody (BD34) inhibited aggregation of WT and Ero1α-null platelets (Figure S8E). Using intravital microscopy, we found that injection of 15E9 into mice did not reduce platelet thrombus formation and fibrin generation at the site of laser-induced cremaster arteriolar thrombosis (Figure 2K–L). In contrast, inhibition of extracellular Pdi significantly blocked both events. Taken together, these results indicate that intracellular ERO1α promotes platelet activation and aggregation independently of PDI activity.

Platelet ERO1α contributes to Ca^{2+} content and enhances Ca^{2+} mobilization by modifying an allosteric disulfide bond in STIM1 and SERCA2

To determine how ERO1α regulates platelet function, we first performed mass spectrometry to identify its binding molecules. ERO1α interacted with many molecules, including PDI family member thiol isomerases, SERPINs, and Ca^{2+} signaling molecules, such as STIM1 and sarco/endoplasmic reticulum Ca^{2+}-ATPase 2 (SERCA2) (Figure 3A and Data file S2). The volcano plot showed a significant change in ERO1α binding to its binding molecules, including STIM1 and SERCA2, during platelet activation (Figure 3A). Among them, we focused on STIM1 and SERCA2 since they are crucial for Ca^{2+} signaling which may explain defects in Ero1α-null platelet activation and aggregation induced by multiple agonists. Using immunoprecipitation assays, we confirmed that ERO1α bound to STIM1 and SERCA2 (Figure 3B–C). Intriguingly, thrombin treatment significantly increased ERO1α binding to STIM1 but reduced its binding to SERCA2 in human platelets without affecting the ERO1α amount.

As assessed by the fluorescence-based FLIPR Ca^{2+} assay,[25] we found that compared to WT platelets, Ero1α-null platelets exhibited a significant decrease in both Ca^{2+} release and influx after stimulation with thrombin and A23187 (Figure 3D–E). Similar results were obtained in the presence of $CaCl_2$ (Figure S9). Loss of platelet Ero1α reduced Ca^{2+} release and influx induced by thapsigargin (TG), an inhibitor of SERCA (Figure 3F). The decrease in agonist-induced Ca^{2+} mobilization in Ero1α-null platelets did not result from the alteration in dye loading or quenching since WT and Ero1α-null platelets were labeled with calcein AM equivalently (Figure S10). Deletion of platelet Pdi did not affect agonist-induced Ca^{2+} mobilization (Figure S11). These results indicate that platelet Ero1α regulates Ca^{2+} store content and promotes SOCE in a PDI-independent manner. Although EN460 diminished Ca^{2+} release and influx upon A23187 stimulation, the compound increased the basal level of cytosolic Ca^{2+} in a concentration-dependent manner (Figure S12).

PDI is reported to localize in the DTS of platelets.[33,34] Immunogold electron microscopy using a monoclonal anti-PDI antibody (1D3) and a monoclonal anti-ERO1α antibody (10C1) revealed that ERO1α was found with PDI in the DTS in resting and activated human platelets, and no ERO1α was detected on the platelet surface (Figure 3G). It is reported that deletion of platelet STIM1 reduces Ca^{2+} store content in the DTS and SOCE.[4] Thus, we investigated whether ERO1α regulates STIM1 function. We first performed bio-layer interferometry using a biosensor coupled with biotinylated ERO1α and a different concentration of wt or mutant STIM1 in which Cys49 and Cys56 residues were mutated to Ser49 and Ser56 (mSTIM1-Cys49/56Ser). We found that ERO1α directly bound to

wtSTIM1 in a concentration-dependent manner, with a K_D value of 2.6 μM, whereas binding of ERO1α to mutant STIM1 was minimal and not concentration-dependent (Figure 3H), providing no meaningful K_D value. These results indicate that the Cys49 and Cys56 residues in STIM1 are critical for ERO1α binding.

S-nitrosylation at Cys49 and Cys56 residues induces a conformational change in STIM1 and suppresses Ca^{2+} depletion-dependent oligomerization,[35,36] suggesting that a Cys49-Cys56 disulfide bond is likely to have an allosteric function. Thus, we hypothesized that ERO1α regulates the Cys49-Cys56 disulfide bond in STIM1 and its function. Using a pull-down assay with N^{α}-(3-maleimidylpropionyl) biocytin (MPB) reacting with free thiols,[8] we found that the level of free thiol groups in STIM1 was decreased in human and WT mouse platelets upon thrombin stimulation (Figure 3I–J). However, such a decrease in the free thiol level was not observed in activated Ero1α-null platelets (Figure 3K). Mass spectrometry revealed that wtERO1α, but not mERO1α, decreased N-ethylmaleimide (NEM) labeling on the Cys49 residue in STIM1 in a concentration-dependent manner (Figure 3L–N). However, the trypsin-digested Cys56-containing peptide, IDKPL**C**HSEDEK, was not detected probably due to the presence of acidic amino acids which might affect trypsin digestion. Our results provide the first evidence that ERO1α directly interacts with STIM1 and oxidizes the allosteric Cys49-Cys56 disulfide bond, contributing to Ca^{2+} store content and promoting SOCE during platelet activation.

Since ERO1α also interacts with SERCA2 in platelets (Figure 3C), we examined their direct interaction using recombinant proteins. Pull-down assays showed that ERO1α bound to wtSERCA2 (Figure 3O). A recent study demonstrated that oxidation or reduction of the intraluminal Cys875-Cys887 disulfide bond controls the ATPase pump activity of SERCA2.[37] We found that ERO1α binding to mutant SERCA2 in which Cys875 and Cys887 residues were replaced with Ser875 and Ser887 (mSERCA2-Cys875/887Ser) was significantly reduced compared to wtSERCA2. Nevertheless, we could not detect MPB-labeled SERCA2 in platelets (Figure S13). As assessed by mass spectrometry using purified proteins, wtERO1α, but not mERO1α, increased NEM labeling on the Cys875 residue in SERCA2 (Figure 3P–Q). The trypsin-digested Cys887-containing peptide, EDNPDFEGVD**C**AIFESPYPMTMALSVLVTIEMCNALNSLSENQSLLR, was not detected because it is too long. This result suggests that the Cys875 and Cys887 residues in SERCA2 are important for ERO1α binding and implies that ERO1α plays a role in altering the Cys875-Cys887 disulfide bond.

Novel small-molecule ERO1α inhibitors recapitulate the defects in Ero1α-null platelets

Since deletion of Ero1α significantly inhibits thrombus formation at sites of arteriolar and arterial injury without affecting tail bleeding times (Figure 1), we posited that targeting ERO1α with small-molecule inhibitors might be an effective strategy to treat thrombotic diseases. Although EN460 has been used in cell-based studies at a concentration of 5–50 μM,[11,18,38,39] the compound at 3–10 μM significantly inhibited Ero1α-null platelet aggregation and increased the basal Ca^{2+} level in platelets (Figure S7C and S11), which led us to exclude it from our studies. To identify a novel ERO1α inhibitor, we screened 5,800 compounds using an ERO1α activity assay (Figure S14A–B). The assay demonstrated a Z-

factor of 0.73, a signal/noise ratio of 14:1, and a coefficient of variance of 4.4%. Compared with 5 μM EN460, 21 compounds exhibited potent inhibitory effects at 20 μM (Figure S14C). The selected compounds were further tested in assays measuring PDI, antioxidant, and thiol-reacting activities (Figure S14D–F). We identified B12 as an initial hit with an IC_{50} value of 12.4 μM and without affecting PDI, antioxidant, and thiol-reacting activities up to 100 μM (Figure 4A and Figure S14). B12 inhibited P-selectin exposure and αIIbβ3 activation in agonist-activated mouse and human platelets in a concentration-dependent manner (Figure 4B–E).

We then tested 22 derivatives of B12 and identified B12–5 which inhibited ERO1α activity with an IC_{50} value of 7.9 μM and had a minimal effect on H_2O_2, PDI, and thiol-reacting activities at 100 μM (Figure 4F and Table S1). However, B12–5 showed a dose-dependent inhibition on the activity of monoamine oxidase A (MAO-A), another FAD coenzyme, by 30% and 51% at 30 and 100 μM, respectively, without affecting its activity at 10 μM. When B12–5 was docked against ERO1α (PDB: 3AHQ) using Glide within Schrödinger Suite, the phenothiazine head group overlaid well with the tricyclic rings of FAD, forming pi-sulfur interactions with Met389 and Cys397 (Figure 4G). Also, the tail group of B12–5 followed the same path as the alkyl chain in FAD, which formed hydrogen bonds with His255, Asn259, and Arg287. Using bio-layer interferometry, we found that B12–5 directly bound to ERO1α with a K_D value of 12.9 ± 3.8 μM (Figure 4H). B12–5 at 3–10 μM significantly reduced P-selectin exposure and αIIbβ3 activation in mouse and human platelets after stimulation with thrombin or CRP (Figure 4I–L). Importantly, 10 μM B12–5 significantly mitigated thrombin- or CRP-induced WT platelet aggregation without affecting Ero1α-null platelet aggregation (Figure 4M–N), suggesting that B12–5 is a specific inhibitor for ERO1α at least up to 10 μM. We also found that pretreatment of mouse and human platelets with B12–5 dose-dependently inhibited Ca^{2+} release and influx induced by thrombin or A23187 (Figure 4O–R). Overall, we identified B12–5 as an ERO1α inhibitor that recapitulated the defects observed in Ero1α-null platelets.

Targeting Ero1α attenuates the pathogenesis of arterial thrombosis and ischemic stroke without affecting tail bleeding times in mice

To determine the *in vivo* efficacy of B12–5 in arterial thrombosis, we first performed *ex vivo* studies. WT mice were treated with intravenous injection of B12–5, and 1-hour later blood was drawn to measure CBC and isolate platelets. We found that compared to the vehicle control, treatment with B12–5 at 5 μg/g BW significantly inhibited P-selectin exposure, αIIbβ3 integrin activation, and aggregation without affecting CBC (Figure 5A–C and Table 3). A lower dose of B12–5 (2 μg/g BW) did not show inhibitory effects (data not shown), and because of the poor water solubility, we could not test B12–5 at a higher dose. As measured by liquid chromatography-tandem mass spectrometry (LC-MS/MS), the plasma concentration of B12–5 was 346, 88.7, 15.3, 7.3, and 1.6 ng/ml at 5, 15, 30, 60, and 120 minutes, respectively, after intravenous injection of 5 μg/g BW of B12–5 (Figure 5D).

As assessed by intravital microscopy, intravenous injection of B12–5 (5 μg/g BW) into WT mice significantly inhibited platelet thrombus formation but did not affect fibrin generation at the site of laser-induced cremaster arteriolar injury (Figure 5E–F). Consistent with a

previous report,[30] injection of eptifibatide (5 μg/g BW), an αIIbβ3 integrin antagonist, inhibited platelet thrombus formation without reducing fibrin generation. To see the antithrombotic effect of B12–5 in a large artery, the compound was tested in a mouse model of $FeCl_3$-induced carotid arterial thrombosis. Compared to the vehicle control, both B12–5 and eptifibatide significantly prolonged the time to occlusion (Figure 5G). However, treatment with eptifibatide markedly prolonged tail bleeding times and increased blood loss in mice, whereas B12–5 did not affect (Figure 5H–I).

Ischemic stroke results from thrombus-mediated obstruction of cerebral blood flow and subsequent reperfusion injury in which platelets and immune cells contribute to disease pathology.[40] To determine the role of ERO1α in ischemic stroke, we tested megakaryocyte-specific Ero1α CKO and global KO mice in a model of transient middle cerebral artery occlusion (tMCAO for 45 minutes) and subsequent reperfusion (23 hours).[8] Compared to WT control, Ero1α KO mice exhibited a significant reduction in infarct volume after tMCAO and improvement in neurological deficits as assessed by the Bederson score and Grip test (Figure 5J–M). Megakaryocyte-specific deletion of Ero1α minimally affected infarct volume and neurological deficits. Single intravenous injection of 5 μg/g BW of B12–5 into WT (C57BL/6) mice immediately after tMCAO significantly reduced infarct volume and ameliorated neurological deficits compared to vehicle control (Figure 5N–Q). These results suggest that ERO1α may be a potential pharmacological target for treating ischemic stroke.

DISCUSSION

Platelet-released PDI binds to the platelet surface, enhancing the ligand-binding function of platelet surface molecules and promoting thrombogenesis.[8,22] In the present study, we have tested the hypothesis that platelet ERO1α plays a role in arterial thrombosis by regulating extracellular PDI activity. Using a wide range of *in vitro* and *in vivo* studies with Ero1α CKO and KO mice, novel blocking antibodies, and small-molecule inhibitors, we have shown that our hypothesis is incorrect. Instead, we demonstrate that ERO1α is neither released from platelets nor detected on the platelet surface and that deletion or inhibition of Ero1α in mice significantly reduces platelet thrombus formation in arterial thrombosis and infarct volume in ischemic stroke without affecting tail bleeding times. Intracellular ERO1α contributes to Ca^{2+} store content and promotes Ca^{2+} mobilization and platelet activation and aggregation in a PDI-independent manner. Mechanistically, ERO1α directly interacts with STIM1 and SERCA2, oxidizes an allosteric disulfide bond, and regulates their function. Ero1α, unlike Pdi,[11] is dispensable for mouse survival. Treatment of mice with blocking anti-PDI antibodies prolongs tail bleeding times in mice.[7] Therefore, our results suggest that compared to PDI, ERO1α may be a more attractive target for developing an antithrombotic agent.

Pdi is detected at sites of laser-induced arteriolar injury and within developing platelet thrombi in mice. The kinetics of Pdi accumulation correlates with that of platelet accumulation,[7] whereas the kinetics of Ero1α accumulation does not (Figure 1B–C). We have further found that a similar level of extracellular Ero1α is detected at the site of laser injury in WT control and Ero1α CKO mice, but its level is negligible in Ero1α KO mice

(Figure S15). Although ERO1α may be present in circulation, we could not detect plasma Ero1α by immunoblotting with a detection limit of 1 ng/ml (Figure S16). These results suggest that while extracellular Pdi is derived from both laser-damaged cells and aggregating platelets,[7,22,41] extracellular Ero1α is not from platelets and likely from laser-damaged cells. Furthermore, inhibition of extracellular Pdi with blocking anti-PDI antibodies significantly reduces arteriolar thrombogenesis in mice.[7,22] In contrast, treatment of mice with 15E9 does not affect platelet thrombus formation and fibrin generation (Figure 2K–L). Overall, our findings suggest that Ero1α detected at sites of vascular injury has a minimal role in thrombogenesis.

It is reported that platelet-released or surface ERO1α regulates αIIbβ3 integrin function and promotes platelet aggregation through PDI.[18,21] However, the *in vitro* studies used very high concentrations of recombinant PDI and ERO1α which are >1,000 times greater than those found under healthy and disease conditions.[19,20] Furthermore, the authors did not prove whether and how ERO1α is secreted from activated platelets. Using flow cytometry and immunogold electron microscopy, we demonstrate that ERO1α is not detected on the platelet surface or released from activated platelets but localizes exclusively in the DTS (Figure S4 and 3G). Consistently, treatment with 15E9 does not affect platelet activation and aggregation (Figure S8). While the aggregation defect in Pdi-null platelets was restored to the WT level in the presence of recombinant wtPDI,[22] such a rescue effect was not observed in Ero1α-null platelets by exogenously-added wtERO1α or wtPDI (Figure 2F). Moreover, unlike PDI,[22] platelet ERO1α is crucial for platelet activation, Ca^{2+} store content, and SOCE (Figure 2G–H and 3D–F). These results suggest that intracellular ERO1α promotes platelet activation by regulating Ca^{2+} signaling in a PDI-independent manner.

Varga-Szabo et al. have reported that loss of platelet STIM1 contributes to Ca^{2+} store content and impairs Ca^{2+} mobilization induced by thapsigargin.[4] This study also showed that deletion of hematopoietic cell STIM1 in mice prolongs the time to occlusion in $FeCl_3$-induced mesenteric arteriolar thrombosis.[4] We have obtained similar results from Ero1α CKO mice, supporting our finding that platelet Ero1α positively regulates STIM1 function. Growing evidence indicates that a Cys49-Cys56 disulfide bond near the EF-hand 1 domain in STIM1 has an allosteric function. S-nitrosylation at the Cys49 and Cys56 residues suppresses Ca^{2+} depletion-dependent oligomerization of the ER luminal domain and inhibits SOCE in cardiomyocytes and HEK293 cells.[35,36] Furthermore, ERp57 cleaves the Cys49-Cys56 disulfide bond, impairing STIM1-mediated SOCE.[42] We have demonstrated that platelet ERO1α interacts with STIM1 through the Cys49 and Cys56 residues and oxidizes the Cys49-Cys56 disulfide bond during cell activation, thereby contributing to Ca^{2+} store content in the DTS and promoting Ca^{2+} mobilization. Furthermore, loss of STIM1 significantly reduces SOCE in neutrophils stimulated with a Ca^{2+} ionophore.[43] This study may explain how loss of Ero1α impairs SOCE in A23187-stimulated platelets. Overall, our results provide the first evidence that ERO1α-mediated oxidation of the allosteric Cys49-Cys56 disulfide bond positively regulates STIM1 function.

Although STIM1-null platelets show defects in platelet activation and aggregation induced by CRP but not ADP or thrombin,[4] Ero1α-null platelets exhibit the functional defect after stimulation with CRP and thrombin (Figure 2B–C and 2G–H). This result suggests that the

regulatory function of ERO1α is not limited to STIM1. It is reported that the pump activity of SERCA2 is inhibited by ERp57-mediated oxidation of a Cys875-Cys887 disulfide bond in the intraluminal loop 4 and is enhanced by ERdj5-mediated cleavage of the disulfide bond.[37,44] We have found that ERO1α interacts with SERCA2 and that their binding depends on Cys875 and Cys887 residues in SERCA2 (Figure 3C and 3O). Surprisingly, mass spectrometric analysis shows increased NEM labeling on Cys875 in the presence of wtERO1α (Figure 3P–Q). Since Cys875 and Cys887 residues are already oxidized in recombinant SERCA2 and ERO1α acts as an oxidase but not a reductase, this may be due to a transient disulfide bond between ERO1α and the Cys875 or Cys887 residue in SERCA2. In addition, our mass spectrometry combined with immunoprecipitation shows that ERO1α may interact with inositol triphosphate receptors (IP3Rs) (Data file S2) that induce Ca^{2+} release after thrombin stimulation. It is reported that ERO1α stimulates IP3Rs during macrophage apoptosis[45] and that IP3R function is regulated by thiol modification.[46] Although we observed the increased ERO1α-IP3Rs in activated platelets (Figure S17), we could not identify the mechanism due to the difficulty of expressing this high molecular weight protein (320-kDa). Further studies are required to investigate whether ERO1α regulates the function of IP3Rs after thrombin stimulation.

Studies suggest that EN460 inhibits not only ERO1α (IC_{50} = 1.9 μM) but also other FAD-containing enzymes, including MAO-A (IC_{50} = 7.9 μM) and MAO-B (IC_{50} = 30.6 μM),[38] and has thiol-reacting activity.[32] Furthermore, the compound at 3 μM completely blocked agonist-induced Ero1α-null platelet aggregation (Figure S7C). In contrast, B12–5 did not show an additional effect on Ero1α-null platelet aggregation up to 10 μM (Figure 4M–N), suggesting a specific inhibitory effect on Ero1α. Although the high concentration (100 μM) of B12–5 did not affect antioxidant, PDI, and thiol-reacting activities, it inhibited MAO-A activity (Table S1) which may affect platelet aggregation.[47,48] In addition, since there is a high sequence homology (around 65%) in the FAD binding pocket of ERO1α and ERO1β, our compound is likely to inhibit the activity of both ERO1 isoforms. Future studies are required to identify more selective and potent ERO1α inhibitors.

We have found that one intravenous injection of B12–5 or eptifibatide into mice inhibits platelet thrombus formation without affecting fibrin generation at the site of laser-induced cremaster arteriolar injury (Figure 5E–F). Our finding that the *ex vivo* and *in vivo* effects of B12–5 on platelet activation and aggregation are maintained at least for 1 hour after injection (Figure 5) suggests that B12–5 gets into circulating platelets and exhibits the effect. In addition to immune cells, platelets play a role in the pathology of ischemic stroke.[49] Despite our understanding of disease pathology, ischemic stroke remains a major cause of death and disability in the U.S., and there is no effective therapy. We have found that deletion of Ero1α and a single intravenous injection of B12–5 after tMCAO significantly reduces infarct volume and improves neurological deficits in a mouse model of ischemic stroke, whereas megakaryocyte-specific deletion of Ero1α has a minimal effect (Figure 5J–Q). These results imply that brain and intravascular cell Ero1α may contribute to the pathogenesis of ischemic stroke. Further studies are required to determine the role of other cellular ERO1α in ischemic brain injury.

Overall, we have identified platelet ERO1α as a novel regulator of Ca^{2+} signaling during platelet activation. Our study demonstrates proof of principle that targeting ERO1α may be a potential therapeutic strategy for preventing or treating thrombotic diseases, such as atherothrombosis and ischemic stroke.

Supplementary Material

Refer to Web version on PubMed Central for supplementary material.

Acknowledgments

The authors thank Dr. R. Reid Townsend and Ernesto Gonzales for their technical assistance.

Sources of Funding

This work was in part supported by grants from the National Institutes of Health (R01HL146559, R01HL130028, R01HL148280, and R01HL153047 to JC, R35HL150797 to XD, and R35HL161175 to JEI). The Washington University Proteomics Shared Resource (WU-PSR) is supported in part by the WU Institute of Clinical and Translational Sciences (NCATS UL1 TR000448), the Mass Spectrometry Research Resource (NIGMS P41 GM103422; R24GM136766) and the Siteman Comprehensive Cancer Center Support Grant (NCI P30 CA091842). The Hope Center for Neurological Disorders is supported in part by the Washington University Institute of Clinical and Translational Sciences grant UL1TR002345 from the National Center for Advancing Translational Sciences (NCATS) of the National Institutes of Health. T.K. is a recipient of the American Heart Association Postdoctoral Fellowship (POST1011698).

Non-standard Abbreviations and Acronyms

AUC	Area under the curve
BW	Body weight
CBC	Complete blood counts
CKO	Conditional knockout
CRP	Collagen-related peptides
DTS	Dense tubular system
ERO1α	Endoplasmic reticulum oxidoreductase 1α
GP	Glycoprotein
IP3R	Inositol triphosphate receptor
LC-MS/MS	Liquid chromatography-tandem mass spectrometry
MAO-A	Monoamine oxidase A
MPB	N^{α}-(3-maleimidylpropionyl) biocytin
NEM	N-ethylmaleimide
PDI	Protein disulfide isomerase
SERCA	Sarco/ER Ca^{2+} ATPase

STIM1	Stromal interaction molecule 1
tMCAO	Transient middle cerebral artery occlusion
TTO	Time to occlusion
vWF	von Willebrand factor

References

1. Writing Group M, Mozaffarian D, Benjamin EJ, Go AS, Arnett DK, Blaha MJ, Cushman M, Das SR, de Ferranti S, Despres JP, et al. Heart Disease and Stroke Statistics-2016 Update: A Report From the American Heart Association. Circulation 2016;133:e38–360. doi: 10.1161/CIR.0000000000000350 [PubMed: 26673558]
2. Li Z, Delaney MK, O'Brien KA, Du X. Signaling during platelet adhesion and activation. Arterioscler Thromb Vasc Biol 2010;30:2341–2349. doi: 10.1161/ATVBAHA.110.207522 [PubMed: 21071698]
3. Gudlur A, Zeraik AE, Hirve N, Hogan PG. STIM calcium sensing and conformational change. J Physiol 2020;598:1695–1705. doi: 10.1113/JP276524 [PubMed: 31228261]
4. Varga-Szabo D, Braun A, Kleinschnitz C, Bender M, Pleines I, Pham M, Renne T, Stoll G, Nieswandt B. The calcium sensor STIM1 is an essential mediator of arterial thrombosis and ischemic brain infarction. J Exp Med 2008;205:1583–1591. doi: 10.1084/jem.20080302 [PubMed: 18559454]
5. Lopez JJ, Jardin I, Bobe R, Pariente JA, Enouf J, Salido GM, Rosado JA. STIM1 regulates acidic Ca2+ store refilling by interaction with SERCA3 in human platelets. Biochem Pharmacol 2008;75:2157–2164. doi: 10.1016/j.bcp.2008.03.010 [PubMed: 18439569]
6. Becker RC, Sexton T, Smyth SS. Translational Implications of Platelets as Vascular First Responders. Circulation research 2018;122:506–522. doi: 10.1161/CIRCRESAHA.117.310939 [PubMed: 29420211]
7. Cho J, Furie BC, Coughlin SR, Furie B. A critical role for extracellular protein disulfide isomerase during thrombus formation in mice. J Clin Invest 2008;118:1123–1131. [PubMed: 18292814]
8. Li J, Kim K, Jeong SY, Chiu J, Xiong B, Petukhov PA, Dai X, Li X, Andrews RK, Du X, et al. Platelet protein disulfide isomerase promotes glycoprotein Ibalpha-mediated platelet-neutrophil interactions under thromboinflammatory conditions. Circulation 2019;139:1300–1319. doi: 10.1161/CIRCULATIONAHA.118.036323 [PubMed: 30586735]
9. Jasuja R, Passam FH, Kennedy DR, Kim SH, van Hessem L, Lin L, Bowley SR, Joshi SS, Dilks JR, Furie B, et al. Protein disulfide isomerase inhibitors constitute a new class of antithrombotic agents. J Clin Invest 2012;122:2104–2113. doi: 10.1172/JCI61228 [PubMed: 22565308]
10. LaMantia M, Miura T, Tachikawa H, Kaplan HA, Lennarz WJ, Mizunaga T. Glycosylation site binding protein and protein disulfide isomerase are identical and essential for cell viability in yeast. Proc Natl Acad Sci U S A 1991;88:4453–4457. [PubMed: 1840696]
11. Jha V, Kumari T, Manickam V, Assar Z, Olson KL, Min JK, Cho J. ERO1-PDI Redox Signaling in Health and Disease. Antioxid Redox Signal 2021;35:1093–1115. doi: 10.1089/ars.2021.0018 [PubMed: 34074138]
12. Appenzeller-Herzog C, Riemer J, Christensen B, Sorensen ES, Ellgaard L. A novel disulphide switch mechanism in Ero1alpha balances ER oxidation in human cells. EMBO J 2008;27:2977–2987. doi: 10.1038/emboj.2008.202 [PubMed: 18833192]
13. Dias-Gunasekara S, Gubbens J, van Lith M, Dunne C, Williams JA, Kataky R, Scoones D, Lapthorn A, Bulleid NJ, Benham AM. Tissue-specific expression and dimerization of the endoplasmic reticulum oxidoreductase Ero1beta. J Biol Chem 2005;280:33066–33075. doi: 10.1074/jbc.M505023200 [PubMed: 16012172]
14. Awazawa M, Futami T, Sakada M, Kaneko K, Ohsugi M, Nakaya K, Terai A, Suzuki R, Koike M, Uchiyama Y, et al. Deregulation of pancreas-specific oxidoreductin ERO1beta in the pathogenesis

of diabetes mellitus. Mol Cell Biol 2014;34:1290–1299. doi: 10.1128/MCB.01647-13 [PubMed: 24469402]

15. Zito E, Chin KT, Blais J, Harding HP, Ron D. ERO1-beta, a pancreas-specific disulfide oxidase, promotes insulin biogenesis and glucose homeostasis. J Cell Biol 2010;188:821–832. doi: 10.1083/jcb.200911086 [PubMed: 20308425]
16. Zito E, Melo EP, Yang Y, Wahlander A, Neubert TA, Ron D. Oxidative protein folding by an endoplasmic reticulum-localized peroxiredoxin. Mol Cell 2010;40:787–797. doi: 10.1016/j.molcel.2010.11.010 [PubMed: 21145486]
17. Araki K, Inaba K. Structure, mechanism, and evolution of Ero1 family enzymes. Antioxid Redox Signal 2012;16:790–799. doi: 10.1089/ars.2011.4418 [PubMed: 22145624]
18. Wang L, Wang X, Lv X, Jin Q, Shang H, Wang CC, Wang L. The extracellular Ero1alpha/PDI electron transport system regulates platelet function by increasing glutathione reduction potential. Redox Biol 2022;50:102244. doi: 10.1016/j.redox.2022.102244 [PubMed: 35077997]
19. Oliveira PVS, Garcia-Rosa S, Sachetto ATA, Moretti AIS, Debbas V, De Bessa TC, Silva NT, Pereira ADC, Martins-de-Souza D, Santoro ML, et al. Protein disulfide isomerase plasma levels in healthy humans reveal proteomic signatures involved in contrasting endothelial phenotypes. Redox Biol 2019;22:101142. doi: 10.1016/j.redox.2019.101142 [PubMed: 30870787]
20. Sharda AV, Bogue T, Barr A, Mendez LM, Flaumenhaft R, Zwicker JI. Circulating Protein Disulfide Isomerase Is Associated with Increased Risk of Thrombosis in JAK2-Mutated Myeloproliferative Neoplasms. Clin Cancer Res 2021;27:5708–5717. doi: 10.1158/1078-0432.CCR-21-1140 [PubMed: 34400417]
21. Swiatkowska M, Padula G, Michalec L, Stasiak M, Skurzynski S, Cierniewski CS. Ero1alpha is expressed on blood platelets in association with protein-disulfide isomerase and contributes to redox-controlled remodeling of alphaIIbbeta3. J Biol Chem 2010;285:29874–29883. doi: 10.1074/jbc.M109.092486 [PubMed: 20562109]
22. Kim K, Hahm E, Li J, Holbrook LM, Sasikumar P, Stanley RG, Ushio-Fukai M, Gibbins JM, Cho J. Platelet protein disulfide isomerase is required for thrombus formation but not essential for hemostasis in mice. Blood 2013;122:1052–1061. [PubMed: 23788140]
23. Li J, Kumari T, Barazia A, Jha V, Jeong SY, Olson A, Kim M, Lee BK, Manickam V, Song Z, et al. Neutrophil DREAM promotes neutrophil recruitment in vascular inflammation. J Exp Med 2022;219:e20211083. doi: 10.1084/jem.20211083 [PubMed: 34751735]
24. Kim K, Tseng A, Barazia A, Italiano JE, Cho J. DREAM plays an important role in platelet activation and thrombogenesis. Blood 2017;129:209–225. doi: 10.1182/blood-2016-07-724419 [PubMed: 27903531]
25. Kim K, Li J, Tseng A, Andrews RK, Cho J. NOX2 is critical for heterotypic neutrophil-platelet interactions during vascular inflammation. Blood 2015;126:1952–1964. doi: 10.1182/blood-2014-10-605261 [PubMed: 26333777]
26. Zhou J, Wu Y, Wang L, Rauova L, Hayes VM, Poncz M, Essex DW. The C-terminal CGHC motif of protein disulfide isomerase supports thrombosis. J Clin Invest 2015;125:4391–4406. doi: 10.1172/JCI80319 [PubMed: 26529254]
27. Araki K, Iemura S, Kamiya Y, Ron D, Kato K, Natsume T, Nagata K. Ero1-alpha and PDIs constitute a hierarchical electron transfer network of endoplasmic reticulum oxidoreductases. J Cell Biol 2013;202:861–874. doi: 10.1083/jcb.201303027 [PubMed: 24043701]
28. Mezghrani A, Fassio A, Benham A, Simmen T, Braakman I, Sitia R. Manipulation of oxidative protein folding and PDI redox state in mammalian cells. Embo J 2001;20:6288–6296. [PubMed: 11707400]
29. Jamasbi J, Ayabe K, Goto S, Nieswandt B, Peter K, Siess W. Platelet receptors as therapeutic targets: Past, present and future. Thromb Haemost 2017;117:1249–1257. doi: 10.1160/TH16-12-0911 [PubMed: 28597906]
30. Shen B, Zhao X, O'Brien KA, Stojanovic-Terpo A, Delaney MK, Kim K, Cho J, Lam SC, Du X. A directional switch of integrin signalling and a new anti-thrombotic strategy. Nature 2013;503:131–135. doi: 10.1038/nature12613 [PubMed: 24162846]

31. Cho J, Kennedy DR, Lin L, Huang M, Merrill-Skoloff G, Furie BC, Furie B. Protein disulfide isomerase capture during thrombus formation in vivo depends on the presence of beta3 integrins. Blood 2012;120:647–655. doi: 10.1182/blood-2011-08-372532 [PubMed: 22653978]
32. Blais JD, Chin KT, Zito E, Zhang Y, Heldman N, Harding HP, Fass D, Thorpe C, Ron D. A small molecule inhibitor of endoplasmic reticulum oxidation 1 (ERO1) with selectively reversible thiol reactivity. J Biol Chem 2010;285:20993–21003. doi: 10.1074/jbc.M110.126599 [PubMed: 20442408]
33. Thon JN, Peters CG, Machlus KR, Aslam R, Rowley J, Macleod H, Devine MT, Fuchs TA, Weyrich AS, Semple JW, et al. T granules in human platelets function in TLR9 organization and signaling. J Cell Biol 2012;198:561–574. doi: 10.1083/jcb.201111136 [PubMed: 22908309]
34. van Nispen Tot Pannerden HE, van Dijk SM, Du V, Heijnen HF. Platelet protein disulfide isomerase is localized in the dense tubular system and does not become surface expressed after activation. Blood 2009;114:4738–4740. doi: 10.1182/blood-2009-03-210450 [PubMed: 19805615]
35. Gui L, Zhu J, Lu X, Sims SM, Lu WY, Stathopulos PB, Feng Q. S-Nitrosylation of STIM1 by Neuronal Nitric Oxide Synthase Inhibits Store-Operated Ca(2+) Entry. J Mol Biol 2018;430:1773–1785. doi: 10.1016/j.jmb.2018.04.028 [PubMed: 29705071]
36. Zhu J, Lu X, Feng Q, Stathopulos PB. A charge-sensing region in the stromal interaction molecule 1 luminal domain confers stabilization-mediated inhibition of SOCE in response to S-nitrosylation. J Biol Chem 2018;293:8900–8911. doi: 10.1074/jbc.RA117.000503 [PubMed: 29661937]
37. Ushioda R, Miyamoto A, Inoue M, Watanabe S, Okumura M, Maegawa KI, Uegaki K, Fujii S, Fukuda Y, Umitsu M, et al. Redox-assisted regulation of Ca2+ homeostasis in the endoplasmic reticulum by disulfide reductase ERdj5. Proc Natl Acad Sci U S A 2016;113:E6055–E6063. doi: 10.1073/pnas.1605818113 [PubMed: 27694578]
38. Hayes KE, Batsomboon P, Chen WC, Johnson BD, Becker A, Eschrich S, Yang Y, Robart AR, Dudley GB, Geldenhuys WJ, et al. Inhibition of the FAD containing ER oxidoreductin 1 (Ero1) protein by EN-460 as a strategy for treatment of multiple myeloma. Bioorg Med Chem 2019;27:1479–1488. doi: 10.1016/j.bmc.2019.02.016 [PubMed: 30850265]
39. Zhang J, Yang J, Lin C, Liu W, Huo Y, Yang M, Jiang SH, Sun Y, Hua R. Endoplasmic Reticulum stress-dependent expression of ERO1L promotes aerobic glycolysis in Pancreatic Cancer. Theranostics 2020;10:8400–8414. doi: 10.7150/thno.45124 [PubMed: 32724477]
40. De Meyer SF, Langhauser F, Haupeltshofer S, Kleinschnitz C, Casas AI. Thromboinflammation in Brain Ischemia: Recent Updates and Future Perspectives. Stroke 2022;53:1487–1499. doi: 10.1161/STROKEAHA.122.038733 [PubMed: 35360931]
41. Jasuja R, Furie B, Furie BC. Endothelium-derived but not platelet-derived protein disulfide isomerase is required for thrombus formation in vivo. Blood 2010;116:4665–4674. doi: 10.1182/blood-2010-04-278184 [PubMed: 20668226]
42. Prins D, Groenendyk J, Touret N, Michalak M. Modulation of STIM1 and capacitative Ca2+ entry by the endoplasmic reticulum luminal oxidoreductase ERp57. EMBO Rep 2011;12:1182–1188. doi: 10.1038/embor.2011.173 [PubMed: 21941299]
43. Clemens RA, Chong J, Grimes D, Hu Y, Lowell CA. STIM1 and STIM2 cooperatively regulate mouse neutrophil store-operated calcium entry and cytokine production. Blood 2017;130:1565–1577. doi: 10.1182/blood-2016-11-751230 [PubMed: 28724541]
44. Li Y, Camacho P. Ca2+-dependent redox modulation of SERCA 2b by ERp57. J Cell Biol 2004;164:35–46. doi: 10.1083/jcb.200307010 [PubMed: 14699087]
45. Li G, Mongillo M, Chin KT, Harding H, Ron D, Marks AR, Tabas I. Role of ERO1-alpha-mediated stimulation of inositol 1,4,5-triphosphate receptor activity in endoplasmic reticulum stress-induced apoptosis. J Cell Biol 2009;186:783–792. doi: 10.1083/jcb.200904060 [PubMed: 19752026]
46. Kang S, Kang J, Kwon H, Frueh D, Yoo SH, Wagner G, Park S. Effects of redox potential and Ca2+ on the inositol 1,4,5-trisphosphate receptor L3–1 loop region: implications for receptor regulation. J Biol Chem 2008;283:25567–25575. doi: 10.1074/jbc.M803321200 [PubMed: 18635540]
47. Baumgartner HR. 5-Hydroxytryptamine uptake and release in relation to aggregation of rabbit platelets. J Physiol 1969;201:409–423. doi: 10.1113/jphysiol.1969.sp008763 [PubMed: 5780550]

48. Rossi EC, Louis G, Bieber M, Zeller EA. Platelet monoamine oxidase and epinephrine-induced platelet aggregation. Thromb Haemost 1978;40:37–42. [PubMed: 725849]

49. Stegner D, Klaus V, Nieswandt B. Platelets as Modulators of Cerebral Ischemia/Reperfusion Injury. Front Immunol 2019;10:2505. doi: 10.3389/fimmu.2019.02505 [PubMed: 31736950]

Novelty and Significance

What Is Known?

- It is reported that platelet surface ERO1α influences platelet function by regulating the activity of protein disulfide isomerase (PDI).
- Protein activity, in general, are known to be regulated by the modification of allosteric disulfide bond(s).

What New Information Does This Article Contribute?

- Deletion or inhibition of Ero1α in mice reduces platelet thrombus formation in arteriolar/arterial thrombosis and infarct volume in experimental ischemic stroke without increasing tail bleeding times and blood loss.
- Platelet ERO1α localizes exclusively in the dense tubular system and modifies an allosteric disulfide bond in STIM1 and SERCA2, regulating cytosolic Ca^{2+} levels and platelet activation.
- Targeting ERO1α may be a potential strategy to attenuate the pathogenesis of thrombotic diseases.

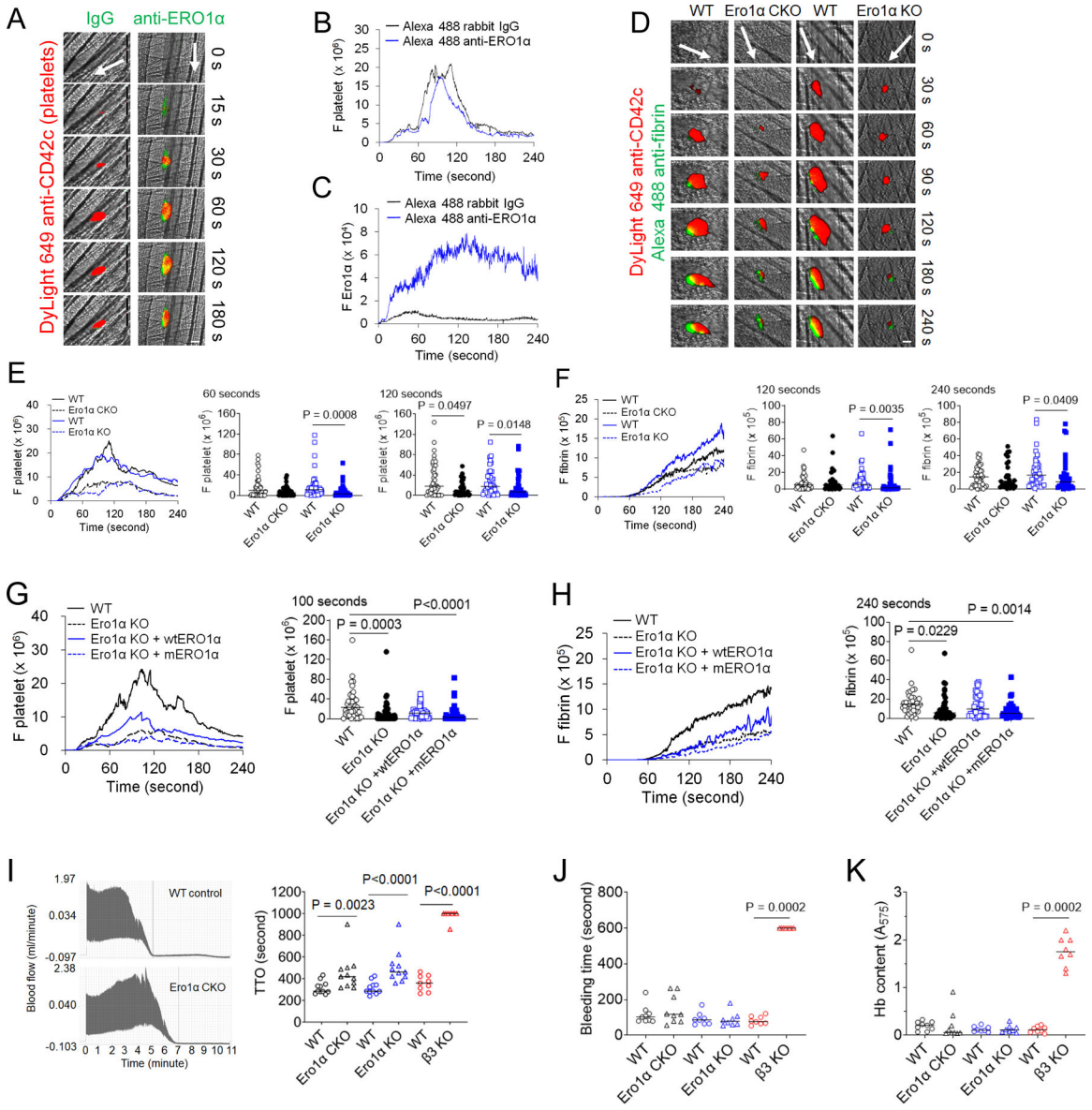

Figure 1. ERO1α has a crucial role in cremaster arteriolar and carotid arterial thrombosis without affecting tail bleeding times in mice.

(A-C) DyLight 649-conjugated anti-CD42c and Alexa 488-conjugated rabbit IgG or polyclonal anti-ERO1α antibodies (0.3 μg/g BW) were injected into WT mice for intravital microscopy. Platelet accumulation and extracellular Ero1α were detected at the site of laser-induced cremaster arteriolar injury. (A) Representative images. (B-C) The median integrated fluorescence intensities of anti-CD42c (F platelet) and anti-ERO1α antibodies (F Ero1α) (n = 41–43 arterioles in 6 WT mice/group). (D-F) Intravital microscopy with WT control and Ero1α CKO and KO mice. After laser-induced cremaster arteriolar injury, platelet accumulation and fibrin generation were detected by injection of DyLight 649-conjugated anti-CD42c and Alexa 488-conjugated anti-fibrin antibodies, respectively. (D) Representative images. (E-F) The median integrated fluorescence intensities of anti-CD42c (F platelet) and anti-fibrin (F fibrin) antibodies (n = 36–44 arterioles in 6 mice/group).

Quantification of the antibody signal at a different time point after laser injury. (G-H) Ero1α KO mice were treated with recombinant wtERO1α or mERO1α (Cys94Ser), 4 μg/g BW. After laser injury, platelets and fibrin were detected as described above (n = 36–38 arterioles in 6 mice/group). (I) The time to occlusion (TTO) was measured by a Doppler blood flow meter in WT control, Ero1α CKO/KO, and β3 KO mice after the application of 6.5% $FeCl_3$ to a carotid artery (n = 8–11 mice/group). (J-K) After amputating the tail tip (5 mm), tail bleeding times and hemoglobin (Hb) contents were measured in WT control, Ero1α CKO/KO, and β3 KO mice (n = 8–9 mice/group). Bars represent the median value. *P* values determined by Mann-Whitney U-test (E-F and I-K) or ANOVA and Dunn's test (G-H).

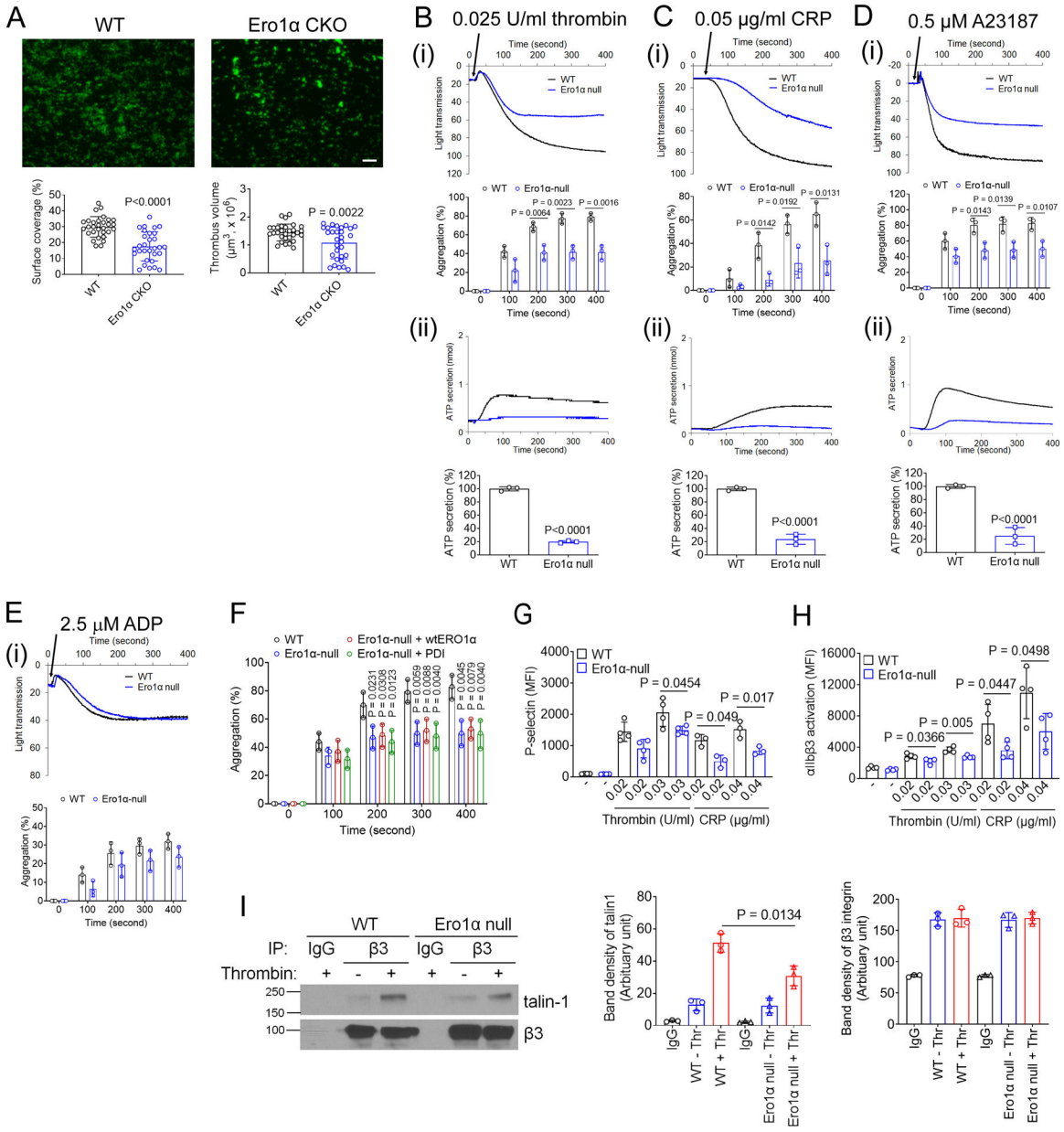

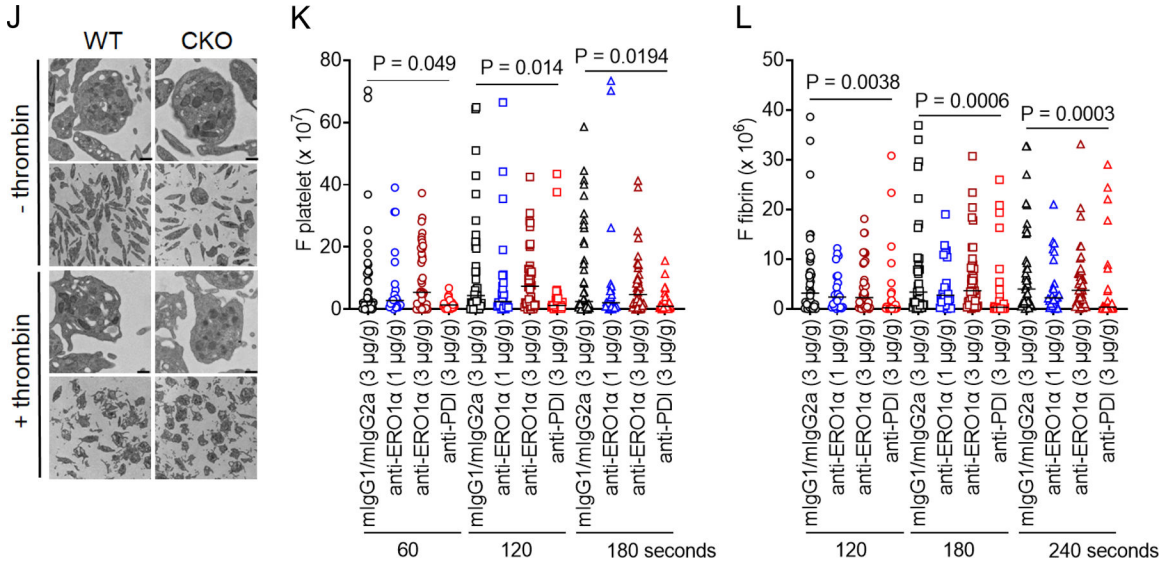

Figure 2. Intracellular ERO1α is crucial for platelet activation, aggregation, and thrombus formation.

(A) *Ex vivo* platelet thrombus formation in a flow chamber assay. Adherent and aggregated platelets were stained with rhodamine-conjugated phalloidin and imaged by confocal microscopy. Representative images (bar = 10 μm). Surface coverage and thrombus volume were measured (mean ± SD, n = 4). (B-E) Aggregation and ATP secretion of WT and Ero1α-null platelets were induced by 0.025 U/ml thrombin, 0.05 μg/ml CRP, 0.5 μM A23187, or 2.5 μM ADP. (i) Platelet aggregation and (ii) ATP secretion. (F) Ero1α-null platelets were pretreated with 50 μg/ml wtERO1α or wtPDI and then with 0.025 U/ml thrombin. Quantification graphs of aggregation and ATP secretion are presented as the mean ± SD (n = 3–4). (G-H) P-selectin exposure and αIIbβ3 integrin activation of WT and Ero1α-null platelets were analyzed by flow cytometry. The data are presented as the geometric mean fluorescence intensity (MFI) value (mean ± SD, n = 3–4). (I) WT and Ero1α-null platelets were treated with or without 0.025 U/ml thrombin for 1 minute in an aggregometer. The lysates were immunoprecipitated with control IgG or anti-β3 antibodies and subjected to immunoblotting with antibodies against talin1 or β3 and densitometric analysis (mean ± SD, n = 3). (J) WT and Ero1α-null platelets were treated with or without 0.025 U/ml thrombin, followed by transmission electron microscopy. The original magnification was 34,800, and the extension was 313,000. Bar = 500 nm. (K-L) Intravital microscopy was performed to determine the effect of 15E9 (1–3 μg/g BW) and a blocking anti-PDI antibody (BD34, 3 μg/g BW) on platelet thrombus formation and fibrin generation at the site of laser-induced cremaster arteriolar injury (n = 27–40 arterioles in 6 mice/group). The n indicates biological replicates. *P* values determined by unpaired Student's *t*-test (A-E and G-I), ANOVA and Dunnett's test (F), or Mann-Whitney U-test (K-L).

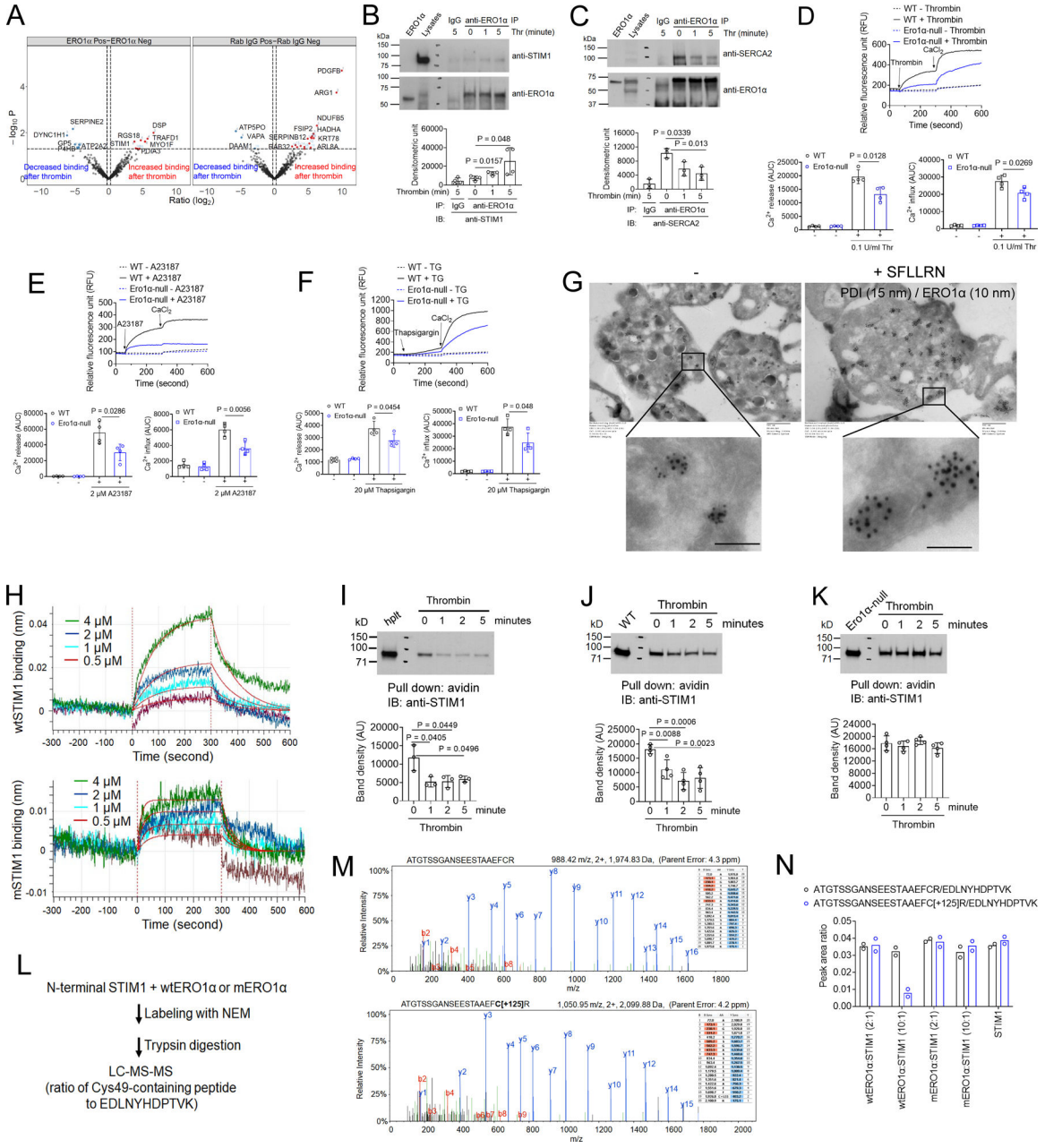

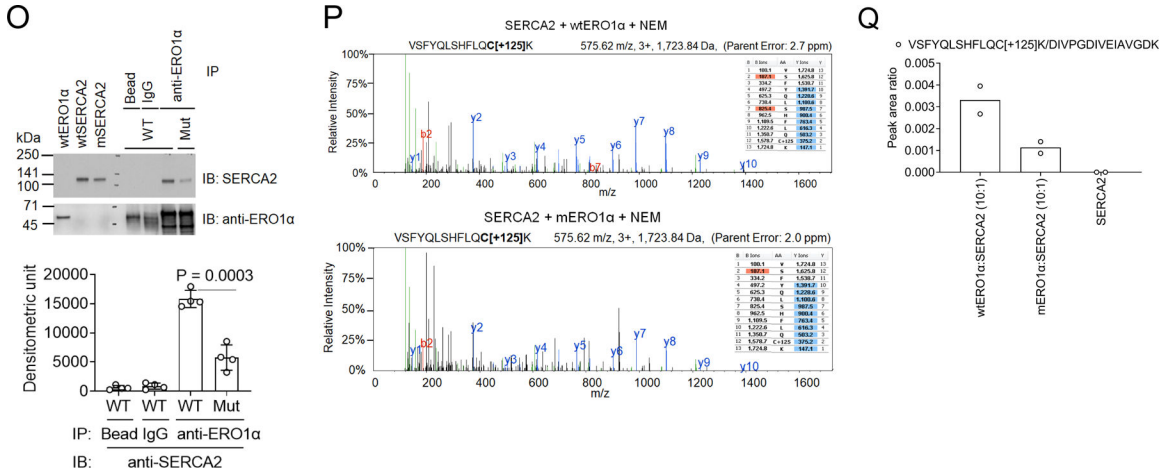

Figure 3. ERO1α regulates the function of Ca^{2+} signaling molecules, STIM1 and SERCA2, and enhances cytosolic Ca^{2+} levels during platelet activation.

(A) Mass spectrometric analysis was performed to identify proteins interacting with ERO1α in resting and thrombin-activated human platelets. Volcano plots show proteins whose binding to ERO1α was significantly increased or decreased during platelet activation. (B-C) Immunoprecipitation of ERO1α with lysates of resting and thrombin (Thr)-activated human platelets, followed by immunoblotting and densitometry. (D-F) Ca^{2+} release and influx of WT and Ero1α-null platelets (CKO) were assessed in response to 0.1 U/ml thrombin, 2 μM A23187, or 20 μM thapsigargin (TG), followed by the addition of 1 mM $CaCl_2$. The Ca^{2+} signal was quantified by the AUC. (G) Immunogold electron microscopy using resting and SFLLRN-activated human platelets. Ultrathin platelet sections were incubated with antibodies against PDI or ERO1α, and bound antibodies were labeled with two different immunogold colloids (15 nm for PDI and 10 nm for ERO1α). (H) Bio-layer interferometry was performed using a biotinylated ERO1α biosensor. After incubation with a different concentration of wtSTIM1 and mSTIM1, the specific interaction between ERO1α and STIM1 was measured by subtracting the non-specific binding. The dissociation constant, K_D, was calculated from the K_{on} and K_{off} values. The data represent the mean ± SD (n = 3). (I-K) Human platelets (hplt) and WT and Ero1α-null platelets were treated with or without 0.025 U/ml thrombin for 0–5 minutes. After labeling the lysates with MPB, proteins were pulled down with streptavidin magnetic beads. The bound fraction was used for immunoblotting with anti-STIM1 antibodies, followed by densitometry. (L) A schematic of mass spectrometric analysis. (M) The representative tandem unmodified and NEM-modified Cys49-containing STIM1 peptides, ATGTSSGANSEESTAAEFCR (988.42 m/z) and ATGTSSGANSEESTAAEFC[+125]R (1,050.95 m/z), respectively. (N) The peak areas for ATGTSSGANSEESTAAEFCR and ATGTSSGANSEESTAAEFC[+125]R were normalized to that of the STIM1 control peptide, EDLNYHDPTVK, which was observed at consistent levels in all samples. (O) WTERO1α was incubated with wtSERCA2 or mSERCA2 (Mut). After immunoprecipitation with polyclonal anti-ERO1α antibodies, the bound fraction was blotted with anti-SERCA2 antibodies, followed by densitometry. (P) The representative tandem NEM-modified Cys875-containing SERCA2 peptide, VSFYQLSHFLQC[+125]K (575.62 m/z). Please note that the unmodified peptide was not detected. (Q) The peak area for the NEM-modified peptide was normalized to that of the SERCA2 control peptide,

DIVPGDIVEIAVGDK, which was observed at consistent levels in all samples. The data represent the mean ± SD (n = 3–4 except N and Q). The n indicates biological replicates. *P* values determined by unpaired Student's *t*-test.

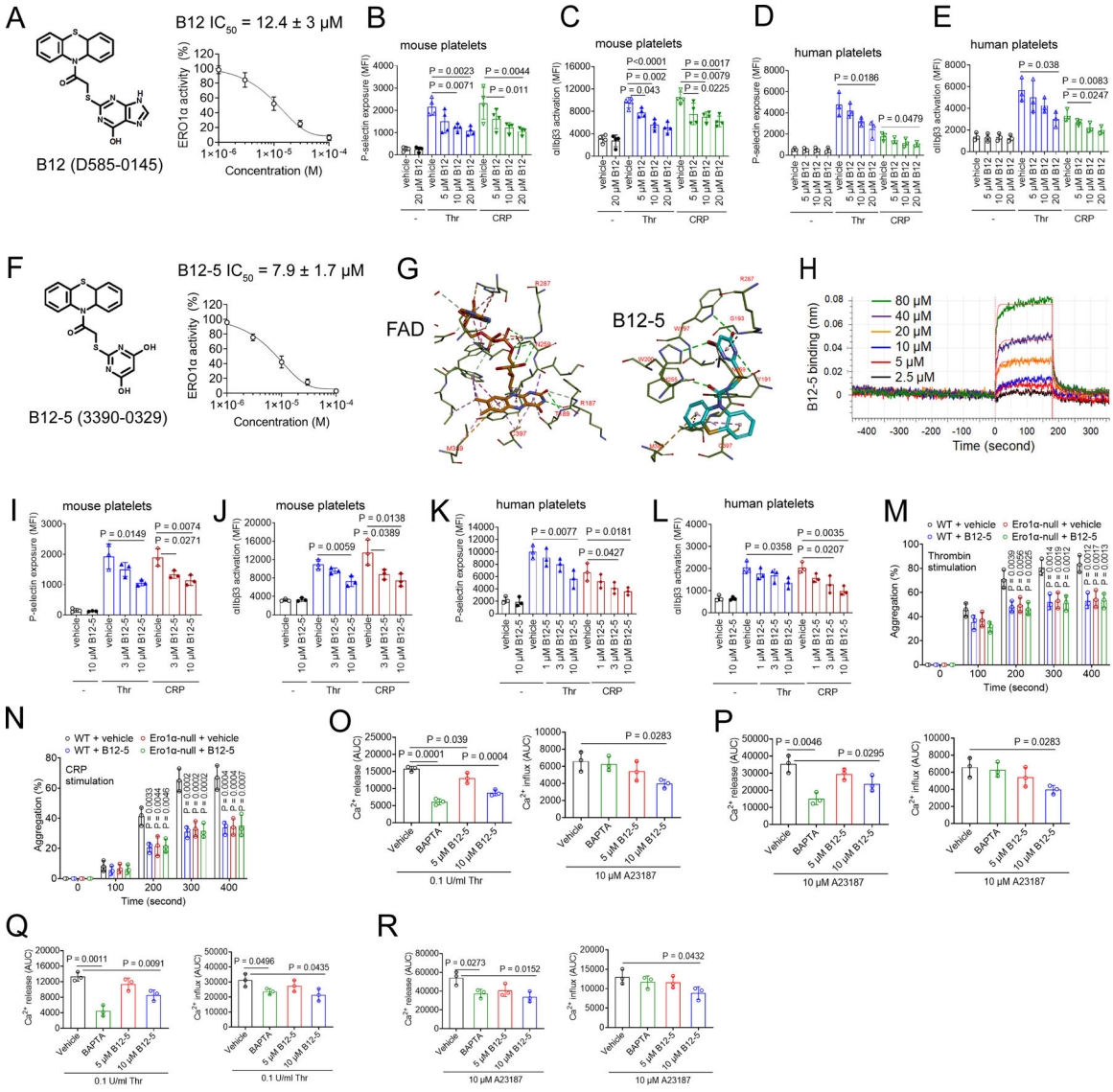

Figure 4. Novel small-molecule inhibitors recapitulate the defect in Ero1α-null platelets.

(A) The structure of B12 and its inhibitory effect on ERO1α activity. (B-E) The inhibitory effect of B12 on P-selectin exposure and αIIbβ3 integrin activation in (B-C) mouse and (D-E) human platelets. (F) The structure of B12–5 and its inhibitory effect on ERO1α activity. (G) A docking model of B12–5-ERO1α (3AHQ) and FAD-ERO1α complex. There are pi-sulfur interactions of the phenothiazine head group (B12–5) or a tricyclic ring (FAD) with Met 389 and Cys397. Also, there are H bond interactions between the tail/alkyl group and His255, Asn259, and Arg287. (H) Bio-layer interferometry was performed using a biosensor conjugated with biotinylated ERO1α. After incubation with a different concentration of B12–5, the specific interaction between B12–5 and ERO1α was measured by subtracting the non-specific binding. The K_D value was calculated from the K_{on} and K_{off} values. The represent trace (n = 3). (I-L) The inhibitory effect of B12–5 on P-selectin exposure and αIIbβ3 integrin activation in (I-J) mouse and (K-L) human platelets. (M-N) The inhibitory effect of B12–5 (10 μM) on WT and Ero1α-null platelet aggregation induced by thrombin

or CRP. (O-R) The effect of B12–5 on Ca^{2+} mobilization in (O-P) mouse and (Q-R) human platelets after stimulation with thrombin or A23187. The data represent the mean ± SD (n = 3–4). The n indicates biological replicates. *P* values determined by ANOVA and Dunnett's test (B-E, I-L, and O-R (for B12–5)) or Student's *t*-test (M-N and O-R (for BAPTA)).

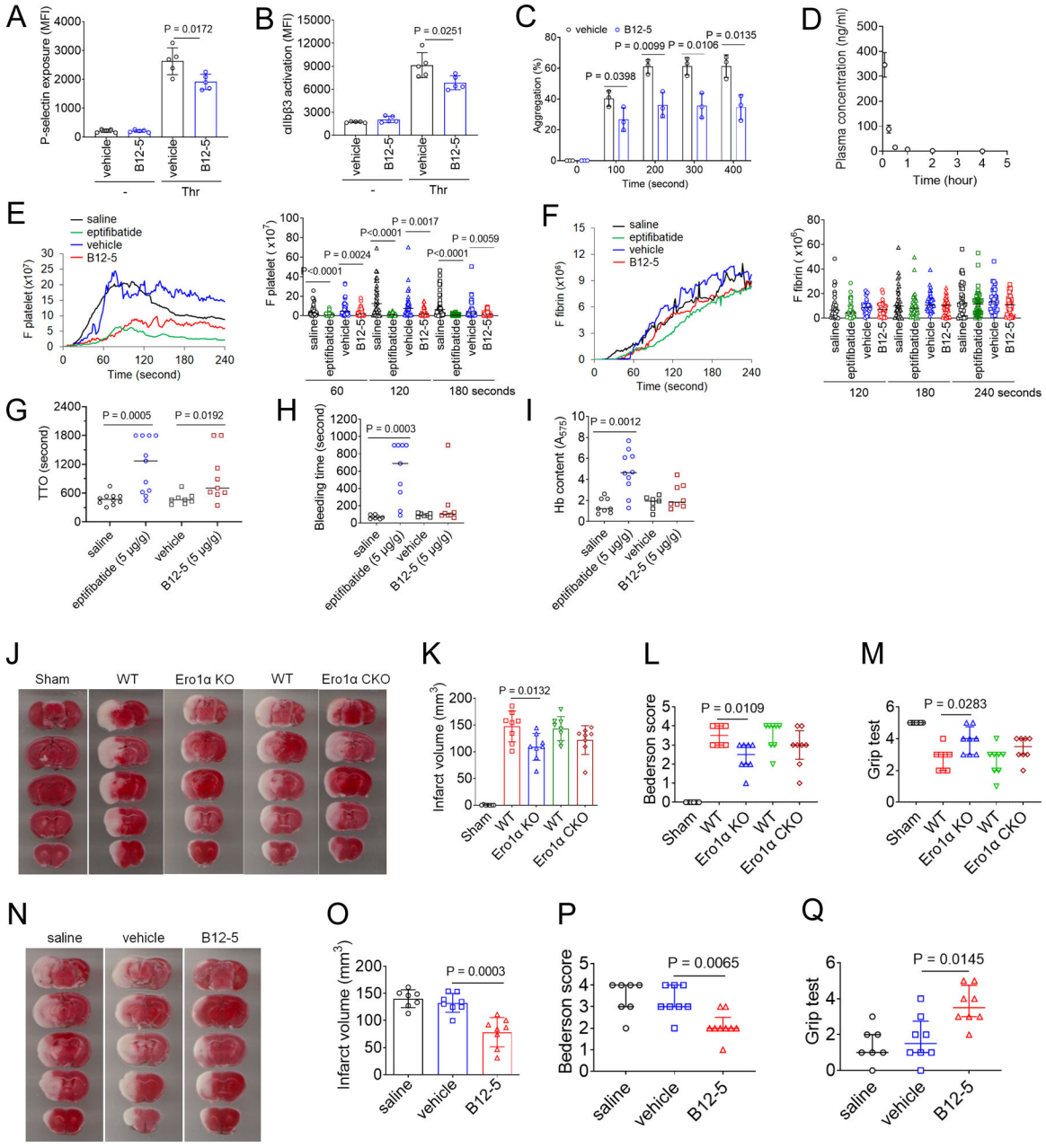

Figure 5. B12–5 has an antithrombotic effect without prolonging tail bleeding times in mice.

(A-C) *Ex vivo* effects of B12–5. WT (C57BL/6) mice were treated with intravenous injection of vehicle (20% PEG + 3% DMSO) or B12–5 (5 μg/g BW). One hour later, blood was drawn, followed by isolating platelets. (A) P-selectin exposure and (B) αIIbβ3 integrin activation were assessed in flow cytometry. (C) Platelet aggregation was measured after treatment with 0.025 U/ml thrombin. The data represent the mean ± SD (n = 4). (D) The plasma levels of B12–5 were analyzed by LC-MS/MS after intravenous injection of the compound (5 μg/g BW) into WT mice and quantified by comparison with a standard curve of B12–5 (mean ± SD, n = 3). (E-F) After laser-induced cremaster arteriolar injury, intravital microscopy was conducted with WT mice pretreated with intravenous injection

of saline, eptifibatide (5 μg/g BW), vehicle, or B12–5 (5 μg/g BW). The median integrated fluorescence intensities of anti-CD42c (F platelet) and anti-fibrin (F fibrin) antibodies (n = 37–42 arterioles in 6 mice/group). Quantification of the antibody signal at a different time point after laser injury. (G) Comparison of B12–5 (5 μg/g BW) with eptifibatide (5 μg/g BW) and their respective controls in inhibiting $FeCl_3$-induced carotid artery thrombosis in WT mice. (H-I) WT mice were treated with intravenous injection of vehicle control, eptifibatide (5 μg/g BW), or B12–5 (5 μg/g BW). Thirty minutes later, tail bleeding times and Hb contents were measured after amputation of the tail tip. Bars represent the median value (E-I). (J-M) WT control and Ero1α CKO and KO mice were subjected to tMCAO. Twenty-three hours later, neurological deficits were assessed by the Bederson score and grip test, and infarct volume was measured as described in Methods. (N-Q) WT mice were subjected to tMCAO and then treated with saline, vehicle, or B12–5 (5 μg/g BW). Twenty-three hours later, the neurological deficit and infarct volume were measured as described above. (K and O) The data represent the mean ± SD (n = 7–8). (L-M and P-Q) The bar indicates the median with interquartile range. *P* values determined by unpaired Student's *t*-test (A-C, K, and O) or Mann-Whitney U-test (E-I, L-M, and P-Q).

Table 1.

CBCs in WT littermate control and Ero1α CKO mice.

	WBC (10^3/μL)	NE (10^3/μL)	LY (10^3/μL)	MO (10^3/μL)	RBC (10^6/μL)	PLT (10^3/μL)	MPV (fL)
WT	7.1 ± 1.9	1.4 ± 0.3	4.2 ± 0.8	0.2 ± 0.1	10.1 ± 0.6	1,208 ± 171	4.9 ± 0.6
Ero1α CKO	6.5 ± 1.4	1.1 ± 0.3	4.3 ± 0.6	0.1 ± 0.0	10.3 ± 0.9	1,128 ± 123	4.4 ± 0.3

Blood cells from mice were counted using HEMAVET 950 (Drew Scientific). The data represent the mean ± SD (n = 8–10 mice (8–12 weeks old) per group).

WBC, white blood cells; NE, neutrophils; LY, lymphocytes; MO, monocytes; RBC, red blood cells; PLT, platelets; MPV, mean platelet volume.

Table 2.

CBCs in WT littermate control and Ero1α KO mice.

	WBC (10^9/L)	NE (10^9/L)	LY (10^9/L)	MO (10^9/L)	RBC (10^{12}/L)	PLT (10^9/L)	MPV (fL)
WT	6.0 ± 1.2	0.8 ± 0.2	4.8 ± 1.1	0.2 ± 0.0	8.6 ± 2.0	1068 ± 220	4.6 ± 0.5
Ero1α KO	5.9 ± 1.1	0.8 ± 0.2	4.9 ± 0.9	0.2 ± 0.1	8.8 ± 1.2	905.3 ± 280	4.6 ± 0.4

Blood cells from mice were counted using HEMAVET 950 (Drew Scientific). The data represent the mean ± SD (n = 8–10 mice (8–12 weeks old) per group).

WBC, white blood cells; NE, neutrophils; LY, lymphocytes; MO, monocytes; RBC, red blood cells; PLT, platelets; MPV, mean platelet volume.

Table 3.

CBCs in vehicle- or B12–5-treated WT mice.

	WBC (10^3/μL)	NE (10^3/μL)	LY (10^3/μL)	MO (10^3/μL)	RBC (10^6/μL)	PLT (10^3/μL)	MPV (fL)
vehicle	5.6 ± 1.0	0.7 ± 0.2	4.5 ± 0.8	0.2 ± 0.1	10.1 ± 1.5	954 ± 156	4.6 ± 0.3
B12–5	5.4 ± 1.1	0.7 ± 0.2	4.2 ± 0.8	0.2 ± 0.1	9.9 ± 1.2	847 ± 114	4.6 ± 0.4

WT (C57BL/6) male mice were treated with intravenous injection of vehicle (20% PEG400 + 3% DMSO) and B12–5 (5 μg/g BW). One hour later, blood was drawn, and cells were counted using HEMAVET 950 (Drew Scientific). The data represent the mean ± SD (n = 6 mice (8–12 weeks old) per group).

WBC, white blood cells; NE, neutrophils; LY, lymphocytes; MO, monocytes; RBC, red blood cells; PLT, platelets; MPV, mean platelet volume.